Int J Cardiovasc Imaging (2014) 30:389–398
DOI 10.1007/s10554-013-0341-4

ORIGINAL PAPER

Sizing the mitral annulus in healthy subjects and patients with mitral regurgitation: 2D versus 3D measurements from cardiac CT

Sonja Gordic · Thi Dan Linh Nguyen-Kim · Robert Manka · Simon Sündermann · Thomas Frauenfelder · Francesco Maisano · Volkmar Falk · Hatem Alkadhi

Received: 21 October 2013 / Accepted: 27 November 2013 / Published online: 4 December 2013

Abstract The purpose of our study was (1) to assess retrospectively, in healthy subjects and in patients with moderate and severe functional mitral regurgitation (FMR), the normal mitral annular dimensions, (2) to determine differences in mitral annular geometry between healthy subjects and patients with FMR, and (3) to evaluate potential errors in 2-dimensional (2D) measurements given the 3D nature of the mitral annulus. 15 patients with no cardiac abnormalities (referred to as *normals*), 13 with moderate and 15 with severe FMR as determined by echocardiography underwent contrast-enhanced cardiac 64-slice Computed tomography (CT) with prospective electrocardiography-gating for excluding coronary artery disease. With an advanced visualization, segmentation, and image analysis software, the area, intercommissural distance (CC), septolateral distance (SLD), and the anterior and posterior circumference of the MA were measured in diastole. We found significant ($P < .001$) differences between normals and patients with severe FMR for area, SLD and posterior circumference in 3D ($P < .001$) and 2D ($P < .001$). Similarly, the SLD and the posterior circumference in both 3D ($P = .002$) and 2D ($P = .001$) were significantly smaller in patients with moderate FMR as compared to those with severe FMR. In contrast, there were no significant differences between groups regarding the CC and the anterior circumference both in 3D and 2D (all, $P > .05$). Measurements in 3D differed significantly from those with 2D for all circumference measurements and groups ($P < .01$), with a systematic underestimation of the posterior circumference of 2.1 ± 1.5 mm in normals, 1.8 ± 1.3 mm in patients with moderate FMR, and 1.9 ± 1.9 mm in patients with severe FMR for 2D. Our study provides in vivo human CT data on MA dimensions in normals and patients with FMR, indicating differences in patients for the area, posterior circumference and SLD but not for the anterior circumference and CC. Systematic differences exist between 2D and 3D measurements for all circumferential measurements.

Keywords Mitral annulus · Circumference · Mitral regurgitation · Computed tomography

S. Gordic · T. D. L. Nguyen-Kim · R. Manka · T. Frauenfelder · H. Alkadhi (✉)
Institute of Diagnostic and Interventional Radiology, University Hospital Zurich, Rämistrasse 100, 8091 Zurich, Switzerland
e-mail: hatem.alkadhi@usz.ch

R. Manka
Clinic for Cardiology, University Hospital Zurich, Zurich, Switzerland

R. Manka
Institute for Biomedical Engineering, University and ETH Zurich, Zurich, Switzerland

S. Sündermann · F. Maisano · V. Falk
Clinic for Cardiovascular Surgery, University Hospital Zurich, Zurich, Switzerland

Introduction

Mitral regurgitation (MR) is the second most common heart valve disease [1]. MR can be the consequence of primary anatomical changes that affect the leaflets and subvalvular apparatus (referred to as organic MR), or can result from left ventricular (LV) remodeling leading to dislocation of papillary muscles and tethering of leaflets in the presence of a morphologically normal valve (referred to as functional MR, FMR) [2]. The most common etiology of organic MR requiring hospitalization in industrialized countries is degenerative mitral valve (MV) disease [3], whereas FMR often occurs in patients with ischemic or idiopathic dilated cardiomyopathy [4].

With increased understanding of the heterogenic pathophysiology of MR, various techniques were developed for the repair of mitral valve disease [5], including minimally invasive approaches [6, 7]. Irrespective of the type of repair and underlying pathology, annuloplasty is an integral part of all procedures for restoring the geometry of the dilated mitral annulus and for enhancing leaflet coaptation [8]. Mitral repair or replacement for FMR in elderly patients with poor LV function is still associated with significant mortality and morbidity [9]. The need for less invasive treatments is driving the field of percutaneous mitral valve interventions, which includes repair and replacement techniques [2, 10, 11].

In contrast to open heart surgery where direct inspection and measurements of the intercommissural distance and the height of the anterior leaflet is easily accomplished, the decision for device selection and planning of the percutaneous approach is based on preprocedural imaging. This imaging information usually is acquired using 2-dimensional (2D) or 3D imaging modalities such as echocardiography (mitral valve anatomy, annular dimensions, spatial relationships) and fluoroscopy (device positioning and monitoring of deployment). However, both echocardiography and fluoroscopy are subject to limitations that might reduce the accuracy of measurements.

Computed tomography (CT) represents a well-established imaging modality in cardiac imaging, providing detailed anatomical 3D-information on both coronary arteries [12] and cardiac valves [13]. Preoperative planning with cardiac CT has shown to be helpful in planning reoperations and minimally invasive cardiac operations [14, 15] and for accurate depiction of the MV apparatus [16–18].

The purpose of this study was (1) to assess retrospectively, in healthy subjects and in patients with moderate and severe FMR, the normal mitral annular dimensions, (2) to determine differences in mitral annular geometry between healthy subjects and patients with FMR, and (3) to evaluate potential errors in 2D measurements given the 3D nature of the mitral annulus.

Materials and methods

Study population

This study was conducted after institutional review board was obtained. Written informed consent was waived because of the retrospective nature of the study.

Between October 2008 and October 2010, 13 patients with moderate FMR (12 male; 69.7 ± 9.6 years; range 53–84 years) and 15 patients with severe FMR (13 male; 65.4 ± 11.1 years; range 47–84 years) as graded by echocardiography were included in our study. Within the same time interval, additional 15 patients who were referred to coronary CT angiography because of a single episode of atypical chest pain were included as the control group (10 male; 69.7 ± 9.6 years; range, 44–77 years). The indication of cardiac CT was the exclusion of coronary artery disease in patients with atypical chest pain having a low to intermediate pre-test probability of coronary heart disease.

Exclusion criteria for CT were nephropathy (serum creatinine level >150 μmol/L), known hypersensitivity to iodine-containing contrast medium, non-sinus rhythm and pregnancy.

All subjects from the control group (subsequently referred to as *normals*) were normotensive (blood pressure, <135/85 mmHg) individuals with sinus rhythm having a low risk for coronary artery disease (based on Framingham criteria [19]). All normals underwent transthoracic echocardiography that showed no abnormalities. Normals had no history of cardiac disease (i.e., myocardial infarction, cardiac surgery, or intervention), no coronary calcifications and no non-calcified atherosclerotic plaques based on calcium scoring and CT coronary angiography, respectively. Catheter angiography was not considered clinically indicated in any of the normals. Exclusion criteria for the control group were electrocardiography (ECG) abnormalities, history of arterial hypertension, and obesity (body mass index (BMI), >30 kg/cm^2).

CT data acquisition and postprocessing

All CT examinations were performed on a 64-section CT machine (Somatom Sensation 64, Siemens Medical Solutions, Forchheim, Germany). The scan range covered the entire heart from the level of tracheal bifurcation to the diaphragm. No β-blockers were administered prior to CT. A bolus of 80 mL of nonionic, iodinated contrast material (Iopromidum, Ultravist 370, 370 mg/mL, Bayer Schering, Berlin, Germany), followed by 30 mL, saline solution was continuously injected into a right antecubital vein via a 18-gauge catheter with an injection rate of 5 mL/s. Contrast agent application was controlled by bolus tracking. A region of interest was placed into the aortic root, and image acquisition started 5 s after the signal density reached the predefined threshold of 140 Hounsfield units (HU). Data acquisition was performed in a cranio-caudal direction with a detector collimation of 32 × 0.6 mm, slice acquisition of 64 × 0.6 mm, gantry rotation time of 330 ms, pitch of 0.2, tube voltage of 120 kV, and tube current–time product of 330 mAs per rotation. The data acquisition was synchronized to the ECG in a prospective mode. Images were reconstructed at a slice thickness of 0.75 mm (increment,

0.5 mm) using a medium-soft tissue convolution kernel (B26f). The mean dose-length-product of our protocol was 170 ± 34 mGy cm equaling an estimated effective radiation dose of 2.9 ± 0.6 mSv [20].

CT data analysis and anatomical definitions

All data were transferred for post-processing to a personal computer (Samsung, SyncMaster 2693 HM) equipped with an advanced visualization, segmentation, and image analysis software (3mensio Structural Heart 6.0, Pie Medical Imaging, Maastricht, NL).

The MA circumference was calculated using the dedicated software by two blinded and independent readers (with 2 and 5 years of experience in cardiovascular imaging, respectively) as follows: After independently placing 16 seed points along the MA (in the long axis reformation), the circumference of the MA both in 3D and 2D (including the anterior and posterior part), the mitral annular area, the intercommissural distance, and the septolateral distance is semiautomatically determined by the software (Figs. 1 and 2). The time effort for the measurements of each CT data set using the dedicated software was on average 5 min. Since the 2D measurements were determined by the software directly from the 3D measurements, the time needed for 2D and 3D measurements was similar.

Definitions of the measurements

Area: is the annulus surface calculated when the annulus is projected to a plane perpendicular through the mathematical center of the mitral annulus.

CC-distance: is the interval between the anterolateral and posteromedial commissures.

SL-distance: is the length at mid-section from the mitro-aortic continuity to the lateral wall, perpendicular to the intercommissural line.

Anterior/Posterior circumference 3D: is the length of the anterior/posterior mitral annular circumference in the 3D space.

Anterior/Posterior circumference 2D: is the length of the anterior/posterior mitral annular circumference in the 3D space projected to a plane perpendicular to the mathematical center.

Entire circumference 3D: anterior circumference 3D + posterior circumference 3D.

Entire circumference 2D: anterior circumference 2D + posterior circumference 2D (see Fig. 1).

Statistical analysis

Quantitative variables were expressed as means ± standard deviations and categorical variables as frequencies or percentages. Variables were assessed for normal distribution using the Kolmogorov–Smirnov test.

To determine the inter-observer agreement between the two readers, the intraclass correlation coefficient (ICC) was calculated for each pair of values. According to Landis and

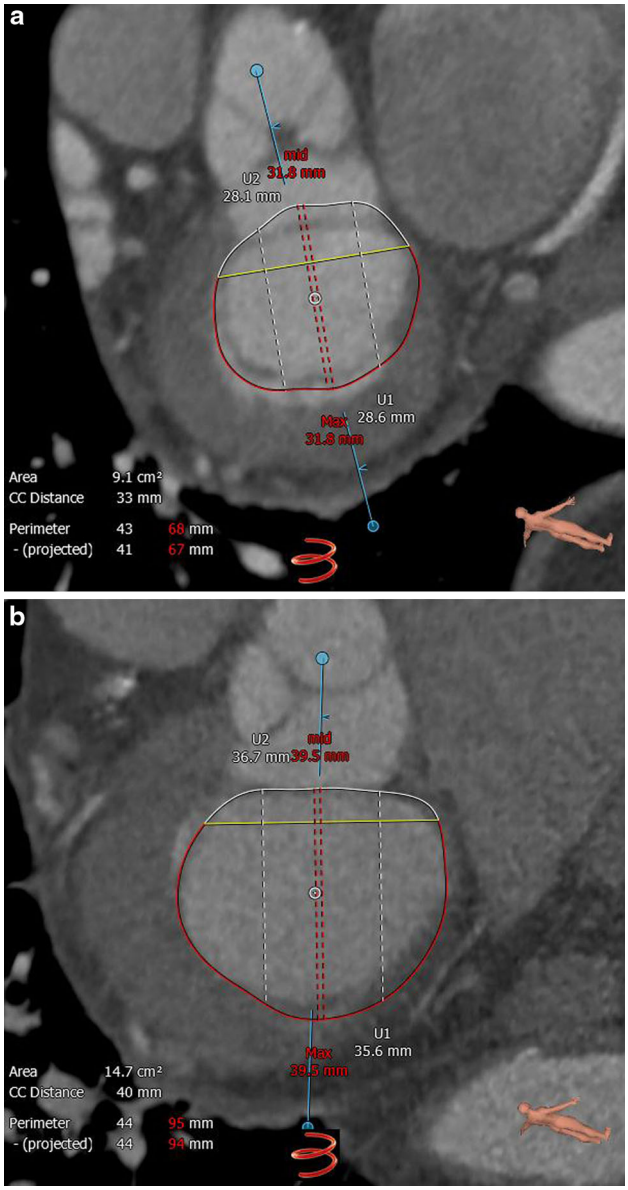

Fig. 1 Measurements in a healthy subject **a** and a patient with severe functional mitral regurgitation **b.** *Turquoise line*: intersection line for the short axis; *yellow line*: intercommissural line; *red broken line* (Max): maximum length from septum to lateral wall; *red broken line* (mid): length at mid-section from septum to lateral wall (i.e. septolateral distance); *white dot*: calculated center of the mitral annular area; *red* and *white color*-coded segments: anterior (*white*) and posterior (*red*) circumference of the MA

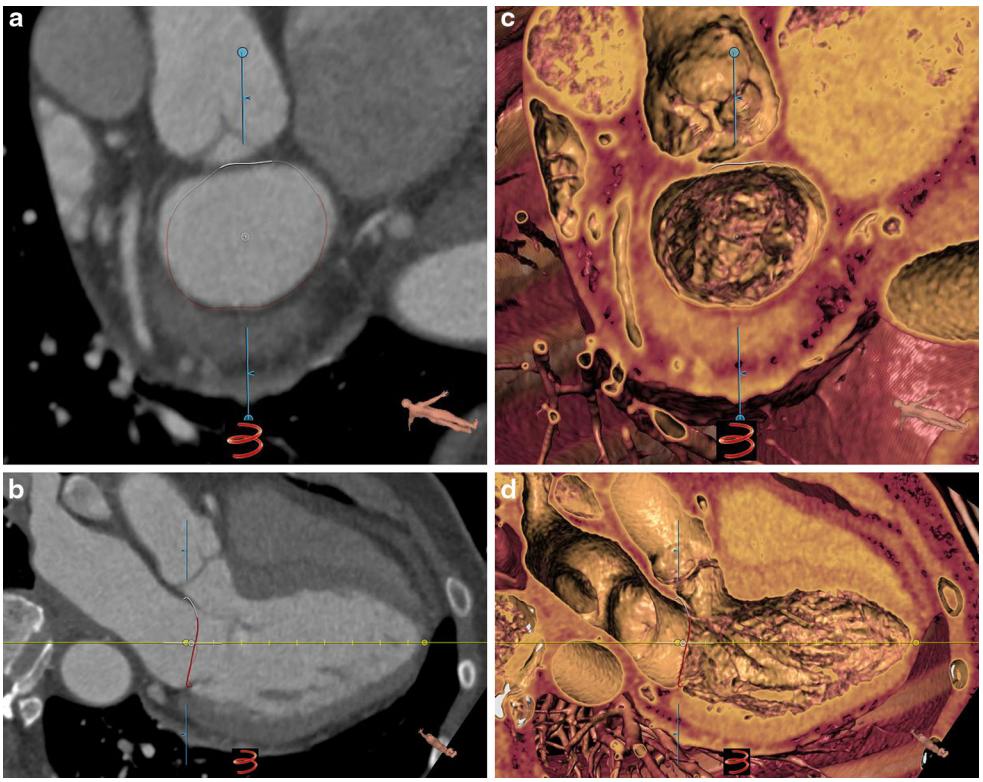

Fig. 2 Short axis (**a** and **c**) and long axis (**b** and **d**) reformation of the mitral valve in a healthy subject in 2D (**a** and **b**) and in 3D (**c** and **d**); *yellow left ventricle-line*: basis for short and long axis reformation created between the two landmarks (perpendicular to the mitral annular area, user placed); turquoise line: intersection line for the short axis reformation; white dot: calculated center of the mitral annular area; red and white color coded segments: anterior and posterior circumference of the MA

Koch, ICC values of .61–.80 were interpreted as substantial, and .81–1.00 as excellent agreement [21].

The Fisher's Exact test was used to compare the gender distribution between the three groups.

One-way Anova analyses with Bonferroni correction for multiple comparisons were performed to test for statistically significant differences in age, area, weight, height, BMI, CC-distance, SL-distance, anterior/posterior circumference, and entire circumference in 3D and 2D.

Comparisons between the 3D and 2D measurements of the annular circumference were tested using the paired *t* test. In addition, Bland–Altman analysis was performed.

All statistical analyses were conducted using commercially available software (SPSS, release 21.0; SPSS, Chicago, IL, USA). A two-tailed P value <.05 was considered to indicate statistical significance.

Results

Patients

There were no significant differences between normals and patients with moderate and severe FMR regarding the age, gender, weight, height and BMI (all, $P > .05$, see Table 1).

Interreader agreement

The interreader agreement was high for all parameters (area: ICC = .983, $P < .001$; CC-distance: ICC = .927, $P < .001$; SL-distance: ICC = .915, $P < .001$; anterior circumference 3D: ICC = .909, $P < .001$; posterior circumference 3D: ICC = .982, $P < .001$; entire circumference 3D: ICC = .974, $P < .001$; anterior circumference 2D: ICC = .947, $P < .001$; posterior circumference 2D: ICC = .979, $P < .001$; entire circumference 2D: ICC = .977, $P < .001$).

Thus, the mean values of the two readers were taken for further analysis.

Measurements

We found significant ($P < .001$) differences between normals and patients with severe FMR for area, SL-distance ($P < .001$) (Fig. 3a), posterior circumference 3D ($P < .001$) and 2D ($P < .001$) (Fig. 3b), as well as for the entire circumference 3D ($P < .001$) and 2D ($P < .001$). There were also significant differences between patients with moderate and severe FMR for SL-distance, the posterior circumference 3D ($P = .002$) and 2D ($P = .001$), as well as for the entire circumference 3D ($P = .001$) and 2D ($P = .001$) (Table 2).

Table 1 Patient demographics

	Patients-overall	Normals (n = 15)	Moderate FMR (n = 13)	Severe FMR (n = 15)	*P* value
Age (mean ± SD) in years	64.2 ± 9.7	69.7 ± 9.6	69.7 ± 9.6	65.4 ± 11.1	0.339
Sex (% male)	81 % (35/43)	66 % (10/15)	92 % (12/13)	87 % (13/15)	0.179
Weight (mean ± SD) in kg	77.1 ± 14.4	80.9 ± 13.2	68.7 ± 13.4	78.4 ± 16.9	0.189
Height (mean ± SD) in m	1.71 ± 6.7	1.73 ± 6.2	1.67 ± 4.1	1.71 ± 9.7	0.214
BMI (mean ± SD) in kg/m2	26.1 ± 4.4	26.9 ± 1.2	24.3 ± 1.6	26.3 ± 1.9	0.459
Ischemic cardiomyopathy	19	0	12	7	NA
Idiopathic dilated cardiomyopathy	9	0	1	8	

FMR functional mitral regurgitation, *SD* standard deviation

In contrast, increases in CC-distance from normals to patients with FMR were not significant (Fig. 3c), and the anterior circumferences were similar in both 3D and 2D among groups (all, $P > .05$) (Fig. 3d).

Comparison of 3D versus 2D measurements

The anterior, posterior and the entire circumferences were significantly different ($P < .001$) comparing 3D with 2D measurements (see Fig. 3b, d). Systematic measurement errors with underestimation of the posterior circumference were 2.1 ± 1.5 mm in normals, 1.8 ± 1.3 mm in patients with moderate FMR, and 1.9 ± 1.9 mm in patients with severe FMR (Fig. 4).

Discussion

This study confirms [17–19] and extends previous knowledge on MA dimensions in normals and in patients with various degrees of FMR. Our results indicate the progressive increases in the MA dimensions (area and circumference) with increasing degrees of FMR are primarily related to dilatations of the posterior MA (as indicated by the SL-distance and posterior circumference) as opposed to the anterior MA (as indicated by the CC-distance and anterior circumference). In addition, we demonstrate systematic errors in determining the mitral annular circumference using 2D- as compared to 3D-approaches with CT, which are explained by the 3D nature of the MA.

Currently, several technologies addressing the MA are under pre-clinical or early clinical evaluation. Under the definition of indirect annuloplasty, all those devices are included that are designed to reshape the annulus without a direct contact, such as coronary sinus implants or cinching devices. Direct annuloplasty refers to a device designed to reproduce a surgical annuloplasty procedure. There are three main direct annuloplasty devices with preliminary clinical experience. The Bident device (Mitralign inc, Tewksbury, USA) in which couples of transannular pledgets are plicated to the posterior annulus in selected locations [22], resembling the surgical key procedure. The Accucinch System (Guided Delivery System, Santa Clara, USA) consists of a subannular implant with multiple anchors, connected by a tethering cable which allows echo-guided posterior annulus remodeling [10]. The Cardioband (ValtechCardio Inc, OrYehuda, Israel) reproduces a posterior surgical band, fixated to the native annulus with a series of helical anchors, which is cinched under echo guidance until sufficient coaptation is restored [23]. All these technologies require a preprocedural assessment of MA anatomy for guiding patient selection and for planning the procedure. In addition to annuloplasty procedures, preprocedural sizing could be critical also in the screening process for transcatheter mitral valve implantation [11].

Studies using human cadaveric hearts with no evident cardiac disease revealed entire MA circumferences between 8.0 and 13.4 cm [24–29]. Different methods of specimen preparation may produce different annular sizes. It is possible that in formalin preserved hearts the annuli are in systolic state, whereas if hearts are fresh or examined after perfusion fixation [29] annuli are in the diastolic state [30]. Using 2D transthoracic echocardiography in healthy humans, Ormiston et al. [30, 31] measured an average entire MA circumference of 9.3 cm (8–10.5 cm) in diastole. Using 3D transesophageal echocardiography in healthy subjects, Khabbaz et al. [32] reported average entire MA circumferences of 11.4 ± 0.5 cm in systole. Using a 3D approach with magnetic resonance imaging in normal healthy subjects, Maffessanti et al. [33] found an average diastolic entire MA circumference of 11.6 cm (11.1–12.5 cm). Our study revealed an average diastolic entire MA circumference of 11.8 ± 0.5 cm for 2D and of 12.3 ± 0.5 cm for 3D in healthy subjects, being in line with previous reports in cadavers, 3D echocardiography and magnetic resonance imaging. The slightly smaller measurements in 2D echocardiography are most probably related to the methods of image analysis, on assumptions of the geometry of the MA, or on the inherent limitations of 2D echocardiography that cannot track distinct anatomic landmarks in time [34].

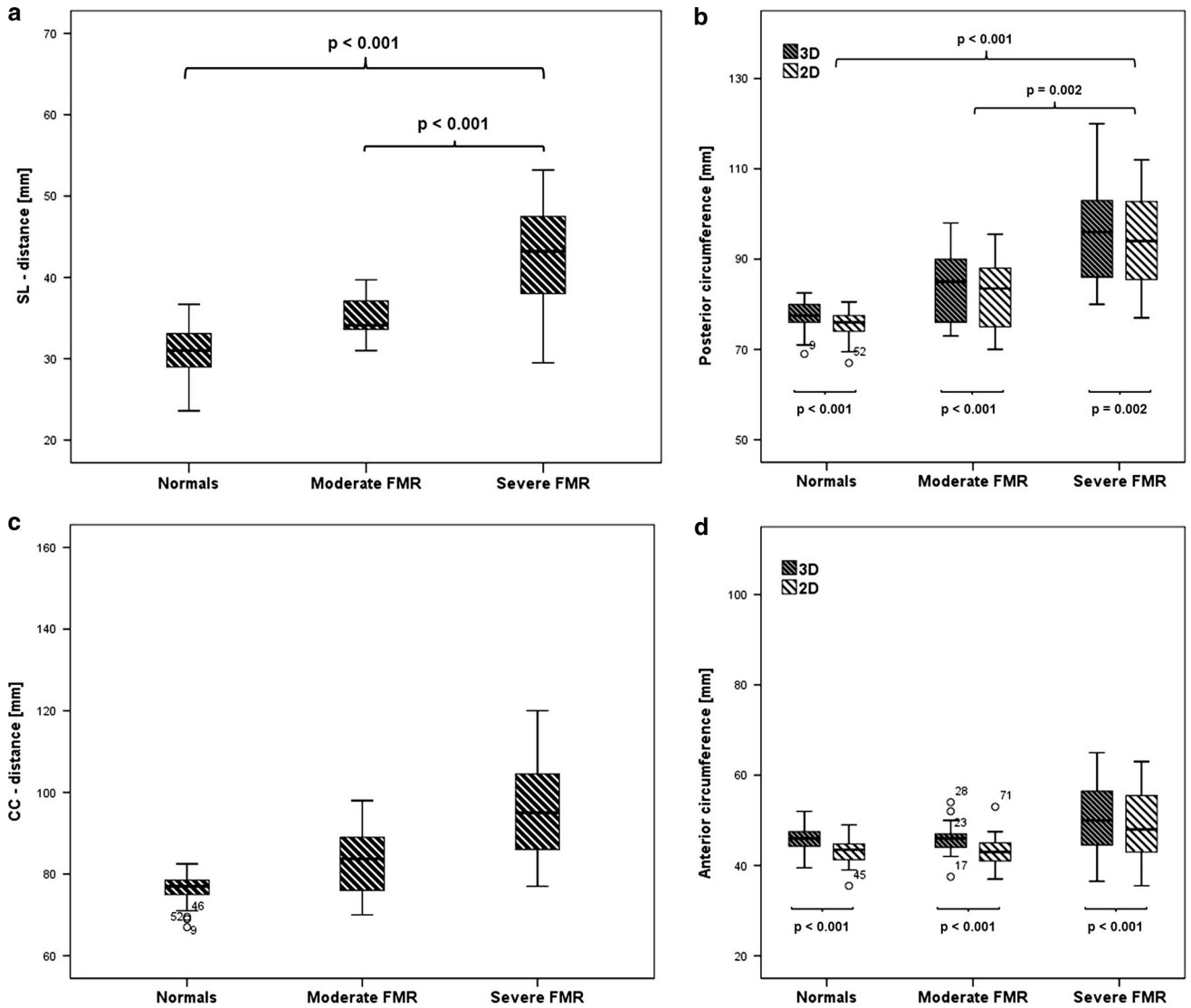

Fig. 3 Boxplots showing measurements of the SL-distance (**a**), posterior circumference (**b**), CC-distance (**c**), and anterior circumference (**d**) between normals and patients with moderate and severe functional mitral regurgitation (FMR). The *horizontal lines* in *boxes* correspond to the median. The *top* and *bottom* of the *boxes* correspond to the second and third quartiles. The *vertical lines* extend to the median ±1.5 times the interquartile range

In patients with both moderate and severe FMR, Khabbaz et al. [32] measured with 3D transesophageal echocardiography an average systolic entire MA circumference of 14.1 ± 0.4 cm. Using a 3D approach with magnetic resonance imaging in patients with various degrees of FMR, Maffessanti et al. [32] reported average diastolic entire MA circumferences of 12.9 cm (11.0–16.3 cm). Our study revealed an average diastolic entire MA circumference of 12.6 ± 0.9 cm for 2D and 13.0 ± 0.8 cm for 3D measurements in patients with moderate FMR and 14.2 ± 1.5 cm for 2D and of 14.6 ± 1.6 cm for 3D measurements in patients with severe FMR.

When comparing 3D with 2D measurements, we found systematic differences in measurements showing systematic underestimations of the posterior circumference ranging between 1.8 and 2.1 mm in normal and patients with FMR. This further highlights the 3D nature of the mitral annulus, which is also a matter of debate regarding the use of flat or flexible annuloplasty devices for surgery and intervention.

It has been reported that the anterior MA due to its fibrous nature is less prone for dilatation [35–37]. The intertrigonal distance may, however, also enlarge, albeit not as much, in long standing FMR as shown in both experimental [38] and human studies [39]. In our study, the anterior circumference and the CC-distances were similar between normal and patients with moderate and severe FMR. On the other hand, in patients with more severe degrees of FMR, the posterior circumference increased significantly that was paralleled by increases of the SL-

Table 2 Values characterizing the mitral annulus in normals and in patients with moderate and severe functional mitral regurgitation (FMR)

	Normals (n = 15)	Patients with moderate FMR (n = 13)	Patients with severe FMR (n = 15)	*P* value
Area (mean ± SD) in cm^2	10.2 ± 1.3*	11.8 ± 1.6	15.4 ± 3.4*	$P < .001$*
CC-distance (mean ± SD) in mm	36.9 ± 3.4	37.4 ± 3.6	40.1 ± 4.6	n.s.
SL-distance (mean ± SD) in mm	30.9 ± 3.4*	35.0 ± 3.0°	42.7 ± 6.5*°	$P < .001$* $P < .001$°
Anterior circumference 3D (mean ± SD) in mm	45.9 ± 3.4	45.8 ± 4.4	50.2 ± 8.6	n.s.
Anterior circumference 2D (mean ± SD) in mm	43.1 ± 3.3	43.2 ± 4.3	48.4 ± 8.5	n.s.
Posterior circumference 3D (mean ± SD) in mm	77.2 ± 3.6*	84.1 ± 7.7°	95.8 ± 11.2*°	$P < .001$* $P = .002$°
Posterior circumference 2D (mean ± SD) in mm	75.2 ± 3.7*	82.3 ± 8.0°	93.8 ± 10.5*°	$P < .001$* $P = .001$°
Entire circumference 3D (mean ± SD) in mm	123.1 ± 4.9*	130.0 ± 7.6°	146.0 ± 16.0*°	$P < .001$* $P = .001$°
Entire circumference 2D (mean ± SD) in mm	118.1 ± 5.2*	125.5 ± 8.7°	142.2 ± 15.3*°	$P < .001$* $P = .001$°

FMR functional mitral regurgitation, *CC-distance* shortest intercommissural distance, *SL-distance* septolateral distance, *SD* standard deviation
Respective *P* values are provided in separate column

* indicates significant difference between normals and patients with severe FMR

° indicates significant difference between patients with moderate and severe FMR

distance. A mismatch between the size of the leaflets and the SL-distance is one of the main mechanisms inducing lack of coaptation in FMR. Our data thus suggest that a procedure for repair of FMR should aim at a shortening of mainly the posterior MA circumference.

Clinical implications

3D echo has been applied for template-based planning in minimally invasive mitral valve repair (mostly degenerative disease) [8, 40, 41]. Pre-operative correlation between the selected ring size with mitral valve assessment and the actual implanted annuloplasty ring size was 0.91 demonstrating that imaging may be useful to guide decision making with regards to the appropriate selection of a mitral ring implant. This study has also shown that superimposition of annuloplasty ring computer-aided design models on the live 3D zoom loops of the mitral valve was superior to 2D measurements of the intercommissural distance or the height of the anterior mitral leaflet, parameters that are routinely used, in predicting correct annuloplasty ring size [40].

As transcatheter annuloplasty and replacement procedures are currently in the early clinical phase, an exact measurement of the annular dimensions preoperatively in will be crucial for appropriate sizing and planning of the procedure. It is therefore of utmost importance to have a reliable tool that can accurately predict the size of the implant.

Recently, it was shown that CT is useful for developing rapid prototyped personalized mitral valve ring implants [42]. This may also apply for the development of percutaneous mitral valve implants. More than 20 different percutaneous mitral valve designs are currently undergoing preclinical studies. Most of the devices are stent based and will rely on "sandwiching" the mitral valve leaflets to anchor stents within the left atrium and the left ventricle [43]. For these devices it will not only be important to determine the annular dimensions but also to define the area of possible landing zones in relation to neighboring structures. CT may play an important role in planning these procedures.

Our study suggests that CT can be used as a planning tool for sizing of MA geometry and in especially the MA circumference before percutaneous catheter-based mitral interventions. It must be noted that CT screening could provide additional critical information for proper procedural planning and device selection (e.g. the shape of the subvalvular apparatus, the distribution of calcium, the location of the coronary arteries, leaflet anatomy).

Currently there are no recommendations or guidelines, to our knowledge, stating which measurement technique (2D or 3D) should be used for clinical routine. This most probably is related to the fact that most of the minimally

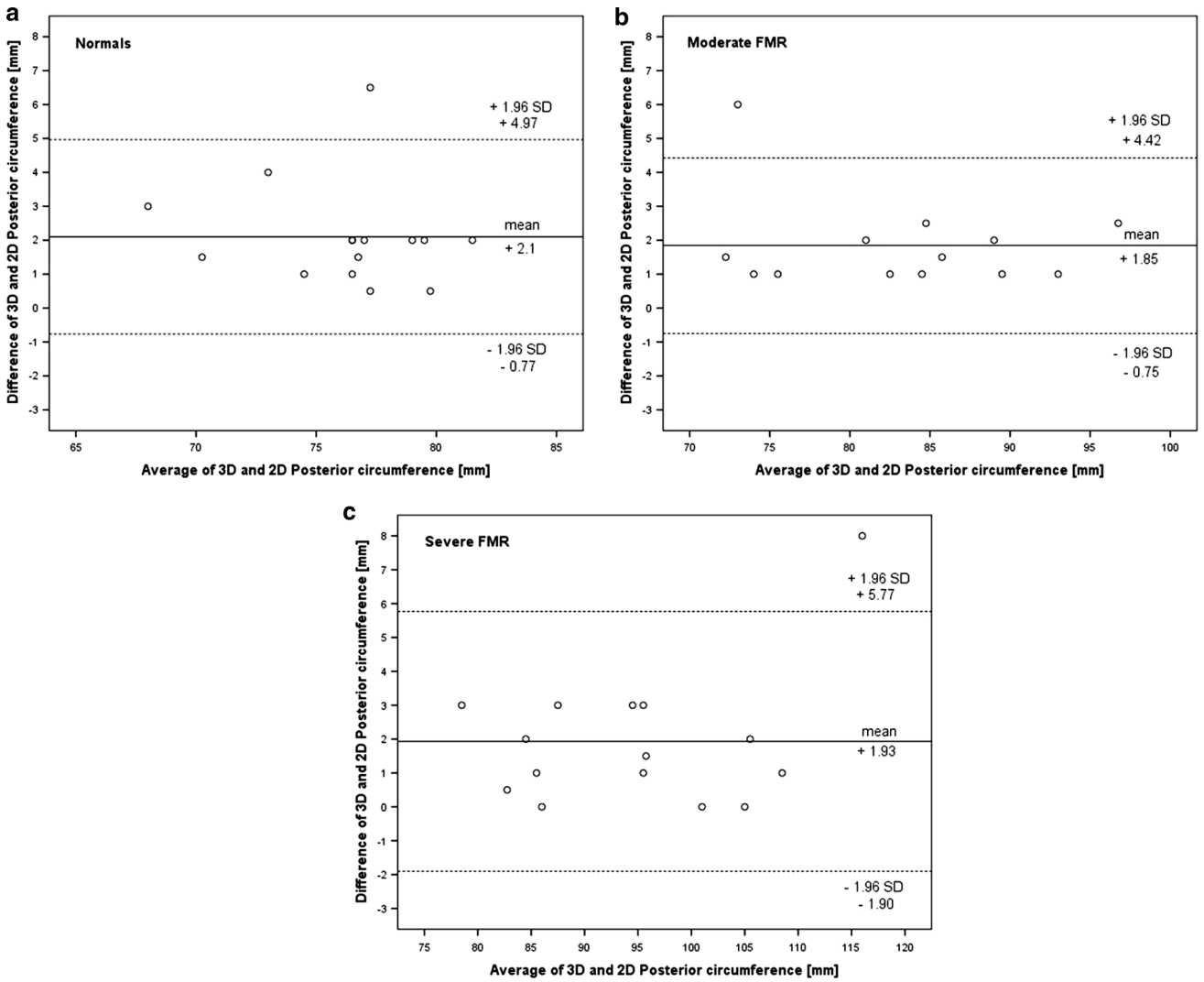

Fig. 4 Bland and Altman analysis demonstrating the agreement between 3D and 2D measurements of the posterior circumference in normals (**a**), in patients with moderate (**b**), and in patients with severe functional mitral regurgitation (**c**). The mean difference between methods (*solid line*) and the limits of agreement (*dashed lines*) are shown

invasive devices mentioned above are not yet widely used in daily clinical routine. Further experience with transcatheter devices in humans will allow for clarification of the issue whether or not 3D measurements are necessary for the precise pre-interventional planning.

Study limitations

The following study limitations must be acknowledged. First, the retrospective nature of our study has inherent shortcomings. Second, we did not include patients with a mild FMR because current guidelines do not support early intervention in this group. Third, we do not have a direct comparison of CT measurements with those from echocardiography. Finally, due to low radiation dose CT protocols used in our study, only images in diastole were available and therefore merely static images of the mitral valve apparatus were obtained. A retrospective spiral data acquisition with 4D reconstructions would be needed for performing measurements in systole and for including the elements of time and motion.

Conclusions

In conclusion, our study provides in vivo human CT data on MA dimensions and circumferences measured in both 2D and 3D in healthy subjects and in patients with FMR. Significant differences exist between patient groups regarding the area, SL-distance and posterior circumference but not regarding the CC-distance and anterior circumference. In addition, systematic differences exist between 2D and 3D measurements for all circumferential measurements.

Conflict of interest Francesco Maisano and Volkmar Falk are consultants for Valtech Cardio Ltd.

References

1. Adams DH, Rosenhek R, Falk V (2010) Degenerative mitral valve regurgitation: best practice revolution. Eur Heart J 31:1958–1966
2. De Bonis M, Maisano F, La Canna G, Alfieri O (2012) Treatment and management of mitral regurgitation. Nat Rev Cardiol 9:133–146
3. Iung B, Vahanian A (2011) Epidemiology of valvular heart disease in the adult. Nat Rev Cardiol 8:162–172
4. Hueb AC, Jatene FB, Moreira LF, Pomerantzeff PM, Kallas E, de Oliveira SA (2002) Ventricular remodeling and mitral valve modifications in dilated cardiomyopathy: new insights from anatomic study. J Thorac Cardiovasc Surg 124:1216–1224
5. Fedak PW, McCarthy PM, Bonow RO (2008) Evolving concepts and technologies in mitral valve repair. Circulation 117:963–974
6. Greelish JP, Cohn LH, Leacche M et al (2003) Minimally invasive mitral valve repair suggests earlier operations for mitral valve disease. J Thorac Cardiovasc Surg 126:365–371 (; discussion 371–373)
7. Nifong LW, Chu VF, Bailey BM et al (2003) Robotic mitral valve repair: experience with the da Vinci system. Ann Thorac Surg 75:438–442 (; discussion 443)
8. Ender J, Koncar-Zeh J, Mukherjee C et al (2008) Value of augmented reality-enhanced transesophageal echocardiography (TEE) for determining optimal annuloplasty ring size during mitral valve repair. Ann Thorac Surg 86:1473–1478
9. Mirabel M, Iung B, Baron G et al (2007) What are the characteristics of patients with severe, symptomatic, mitral regurgitation who are denied surgery? Eur Heart J 28:1358–1365
10. Chiam PT, Ruiz CE (2011) Percutaneous transcatheter mitral valve repair: a classification of the technology. JACC Cardiovasc Interv 4:1–13
11. Banai S, Jolicoeur EM, Schwartz M et al (2012) Tiara: a novel catheter-based mitral valve bioprosthesis: initial experiments and short-term pre-clinical results. J Am Coll Cardiol 60:1430–1431
12. von Ballmoos MW, Haring B, Juillerat P, Alkadhi H (2011) Meta-analysis: diagnostic performance of low-radiation-dose coronary computed tomography angiography. Ann Intern Med 154:413–420
13. Ewe SH, Klautz RJ, Schalij MJ, Delgado V (2011) Role of computed tomography imaging for transcatheter valvular repair/insertion. Int J Cardiovasc Imaging 27:1179–1193
14. Wildermuth S, Leschka S, Duru F, Alkadhi H (2005) 3-D CT for cardiovascular treatment planning. Eur Radiol 15(Suppl 4):D110–D115
15. Cremer J, Teebken OE, Simon A, Hutzelmann A, Heller M, Haverich A (1998) Thoracic computed tomography prior to redo coronary surgery. Eur J Cardiothorac Surg 13:650–654
16. Delgado V, Tops LF, Schuijf JD et al (2009) Assessment of mitral valve anatomy and geometry with multislice computed tomography. JACC Cardiovasc Imaging 2:556–565
17. Alkadhi H, Desbiolles L, Stolzmann P et al (2009) Mitral annular shape, size, and motion in normals and in patients with cardiomyopathy: evaluation with computed tomography. Invest Radiol 44:218–225
18. Deng W, Yang ZG, Peng LQ, Dong ZH, Chu ZG, Wang QL (2010) Morphological and dynamic features of normal mitral valve evaluated by dual-source computed tomography. Int J Cardiol 145:633–636
19. Wilson PWF, D'Agostino RB, Levy D, Belanger AM, Silbershatz H, Kannel WB (1998) Prediction of coronary heart disease using risk factor categories. Circulation 97:1837–1847
20. Alkadhi H, Stolzmann P, Scheffel H et al (2008) Radiation dose of cardiac dual-source CT: the effect of tailoring the protocol to patient-specific parameters. Eur J Radiol 68:385–391
21. Landis JR, Koch GG (1977) The measurement of observer agreement for categorical data. Biometrics 33:159–174
22. Mandinov L (2010) Mitralign Percutaneous Annuloplasty System for the Treatment of Functional Mitral Regurgitation. Eur Cardiol 6(2):67–70
23. Maisano F, Vanermen H, Seeburger J et al (2012) Direct access transcatheter mitral annuloplasty with a sutureless and adjustable device: preclinical experience. Eur J Cardiothorac Surg 42:524–529
24. Gunnal SA, Farooqui MS, Wabale RN (2012) Study of mitral valve in human cadaveric hearts. Heart Views 13:132–135
25. Bulkley BH, Roberts WC (1975) Dilatation of the mitral anulus. A rare cause of mitral regurgitation. Am J Med 59:457–463
26. Rusted IE, Scheifley CH, Edwards JE (1952) Studies of the mitral valve. I. Anatomic features of the normal mitral valve and associated structures. Circulation 6:825–831
27. Chiechi MA, Lees WM, Thompson R (1956) Functional anatomy of the normal mitral valve. J Thorac Surg 32:378–398
28. Duplessis LA, Marchand P (1964) The Anatomy of the Mitral Valve and Its Associated Structures. Thorax 19:221–227
29. McAlpine WA (1975) Heart and Coronary Arteries. Springer Verlag, New York
30. Ormiston JA, Shah PM, Tei C, Wong M (1981) Size and motion of the mitral valve annulus in man. I. A 2-dimensional echocardiographic method and findings in normal subjects. Circulation 64:113–120
31. Levine RA, Handschumacher MD, Sanfilippo AJ et al (1989) Three-dimensional echocardiographic reconstruction of the mitral valve, with implications for the diagnosis of mitral valve prolapse. Circulation 80:589–598
32. Khabbaz KR, Mahmood F, Shakil O et al (2013) Dynamic 3-dimensional echocardiographic assessment of mitral annular geometry in patients with functional mitral regurgitation. Ann Thorac Surg 95:105–110
33. Maffessanti F, Gripari P, Pontone G, et al. (2013) Three-dimensional dynamic assessment of tricuspid and mitral annuli using cardiovascular magnetic resonance. Eur Heart J Cardiovasc Imaging
34. Timek TA, Miller DC (2001) Experimental and clinical assessment of mitral annular area and dynamics: what are we actually measuring? Ann Thorac Surg 72:966–974
35. Otsuji Y, Handschumacher MD, Schwammenthal E et al (1997) Insights from three-dimensional echocardiography into the mechanism of functional mitral regurgitation: direct in vivo demonstration of altered leaflet tethering geometry. Circulation 96:1999–2008
36. Carpentier A, Chauvaud S, Fabiani JN et al (1980) Reconstructive surgery of mitral valve incompetence: 10-year appraisal. J Thorac Cardiovasc Surg 79:338–348
37. Choo SJ, Olomon J, Bowles C et al (1998) An in vitro study of the correlation between aortic valve diameter and mitral intertrigonal distance: a simple method to select the correct mitral annuloplasty ring size. J Heart Valve Dis 7:593–597
38. Tibayan FA, Rodriguez F, Langer F et al (2003) Annular remodeling in chronic ischemic mitral regurgitation: ring selection implications. Ann Thorac Surg 76:1549–1554 (; discussion 1554–1555)
39. Kaji S, Nasu M, Yamamuro A et al (2005) Annular geometry in patients with chronic ischemic mitral regurgitation: three-dimensional magnetic resonance imaging study. Circulation 112:I409–I414
40. Ender J, Eibel S, Mukherjee C et al (2011) Prediction of the annuloplasty ring size in patients undergoing mitral valve repair using real-time three-dimensional transoesophageal echocardiography. Eur J Echocardiogr 12:445–453

41. Bartel T (2013) Contemporary echocardiographic guiding tools for device closure of interatrial communications. Cardiovasc Diagn Ther 3(1):38–46
42. Sundermann SH, Gessat M, Cesarovic N et al (2013) Implantation of personalized, biocompatible mitral annuloplasty rings: feasibility study in an animal model. Interact Cardiovasc Thorac Surg 16:417–422
43. De Bonis M, Maisano F, La Canna G, Alfieri O (2012) Treatment and management of mitral regurgitation. Nat Rev Cardiol 9:133–146